GAP-96-026, Auger project technical note. Self calibration of the water Čerenkov tanks: Simulation

C. Pryke
Enrico Fermi Institute, University of Chicago, USA
email: pryke@hep.uchicago.edu

June 17, 1997

Abstract

An attempt is made to simulate the response of the reference design Auger water Čerenkov detector to the background flux of secondary cosmic rays at ground level. A calculation is developed, and then compared to experimental data.

1 Introduction

It has been suggested that the ever-present flux of ground level background muons will provide a means to calibrate the water tanks of the proposed Auger ground arrays [1] without the use of additional trigger detectors. In the previous paper GAP-97-025 [2] an experimental investigation of this approach was presented. In this companion paper we test how well the AGAsim code [3] can reproduce these results. The experimental data was recorded using the first prototype Auger water tank at AGASA [4], hereafter referred to as AWT1. The realism of the calculation will be improved step-by-step so that we may gauge the impact of the various effects and assumptions.

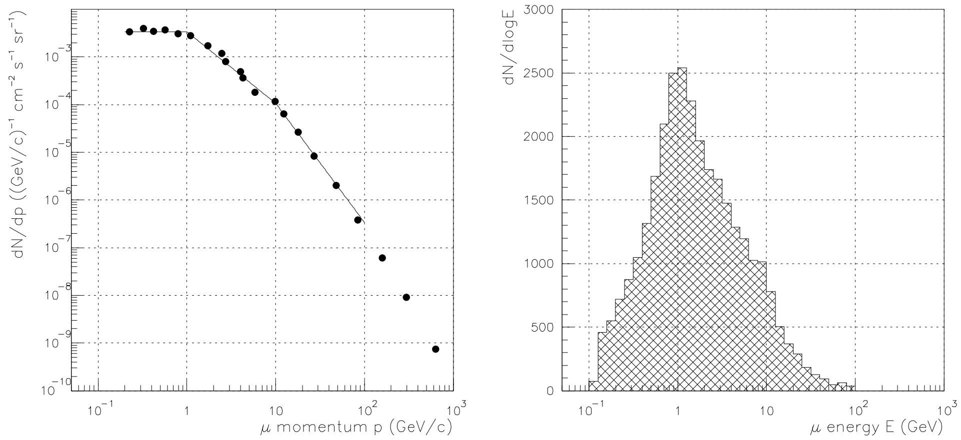

Figure 1: The points on the left are an experimentally measured muon momentum distribution; the lines show a three section power law approximation to the data assumed in this work. At right the resulting kinetic energy distribution is shown.

2 Characteristics of the ground level flux

The total flux of charged particles at ground level crossing the horizontal plane from above is stated in [5] to be $\approx$ 180 s^{-1} m^{-2}. Of these $\approx$ 75% are stated to be penetrating muons, the rest being soft muons and electrons. The fraction of other types is small.

2.1 Energy spectrum

The ground level background muons have a wide spectrum of energies and zenith angles. In the left half of figure 1 dN/dp is plotted, being the differential momentum spectrum of ground level, near vertical muons. The points are taken from [6], and the lines indicate a three section power law approximation to the real spectrum which is used in this work. The right section of the figure indicates the resulting kinetic energy distribution plotted in the form $dN/d\log E$.

Figure 2 shows the rate of direct Čerenkov production by muons moving through water ($n = 1.33$). Čerenkov radiation by δ-ray electrons leads to an increase in light yield over the function shown — this difference grows with

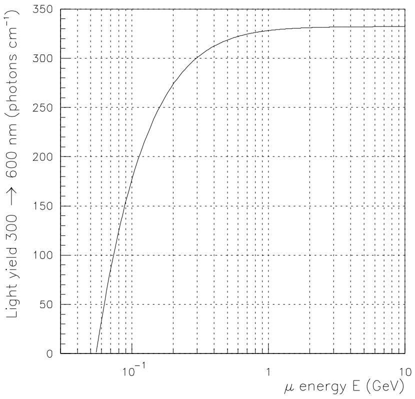

Figure 2: Rate of Čerenkov emission for a muon passing through water, as a function of kinetic energy.

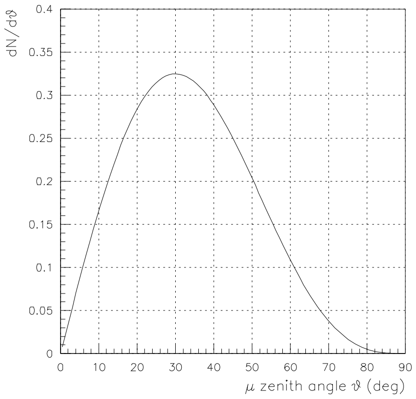

Figure 3: Assumed zenith angle distribution of ground level muons.

energy; in [7] and [8] it is shown to be $\approx 20\%$ at 10 GeV. This effect is not included in AGAsim at this time, although its addition is planned.

Note from figure 1 that the modal $dN/d\log E$ value is approximately 1 GeV. The dN/dp data extends down to 200 MeV/c ($E = 120$ MeV). Below that point the flux is assumed to be zero. Such particles will release little prompt Čerenkov light — however, they will produce decay electrons, and this is possibly important as will be noted latter. An insignificant portion of the flux is at $p > 100$ GeV/c, and these are safely ignored.

The electromagnetic component of the flux is ignored, as are multiple muon (very small air shower) events. These last two are significant shortcomings of the current model.

2.2 Angular distribution

At ≈ 3 GeV the angular distribution of the ground level background muons is stated in [5] to be $\propto \cos^2\theta$; at lower energies it is somewhat steeper, and at higher becomes flatter. We take this to mean that $dN/d\Omega \propto \cos^2\theta$, and hence that for particles crossing the horizontal plane from above $dN/d\theta \propto \cos^3\theta\sin\theta$. Figure 3 shows this function. The correlation between particle energy and zenith angle is ignored in this work.

3 Intersection of particle trajectories with the detector volume

If all muons had high energies, and were hence penetrating, the spread of in-detector track lengths would depend only on the geometry of the tank; specifically on the depth to lateral size ratio. In this work the detector is assumed to be cylindrical with depth 1.2 m, and radius 1.8 m. This corresponds to the dimension of AWT1, and is also the reference design for the Auger detectors [1].

As noted in the introduction, the simulation described here will be developed step by step. Particle start positions are generated in the plane of the detector top surface, and spread randomly over an area with radius $\tan 80^\circ$ times larger than it ($\tan 80^\circ = 5.7$). Zenith angles are sampled from the distribution shown in figure 3. Each particle is then projected forward to determine if its trajectory will intersect the detector volume; if it does the particle is recorded for input to the detector simulation code. In this way corner clipping effects are included, as are particles which enter through the detector side wall. Referring to figure 3 we can see that a negligible fraction of muons have $\theta > 80^\circ$ for the simple assumption made regarding their angular distribution.

Figure 4 is a graphical representation of the above process; a small sample of tracks is shown intersecting the detector. The track length distribution inside the tank is shown in the left part of figure 5. All the simulated distributions in this paper are from runs of 3×10^4 events. Note that a large fraction of tracks are shorter than the modal 1.2 meters ($\approx 30\%$).

4 Adding the muon energy spectrum

Next we include the muon energy spectrum as plotted in the right part of figure 1 and calculate the total Čerenkov light emission in the detector. The right part of figure 5 shows the effect on the track length distribution, while figure 6 shows the distribution of the number of photons released. Note that there is an increase in the fraction of particles whose light emission lies below the peak as compared to the left part of figure 5 (50% as opposed to 30%). This is due to the low-side tail of the muon energy distribution; ie. particles which either stop, or drop below peak Čerenkov light output, while passing through the tank. With the assumption used here that $dN/dp = 0$

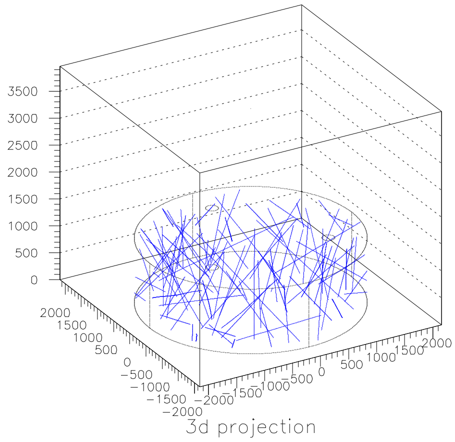

Figure 4: Illustration showing some muon tracks intersecting the detector volume.

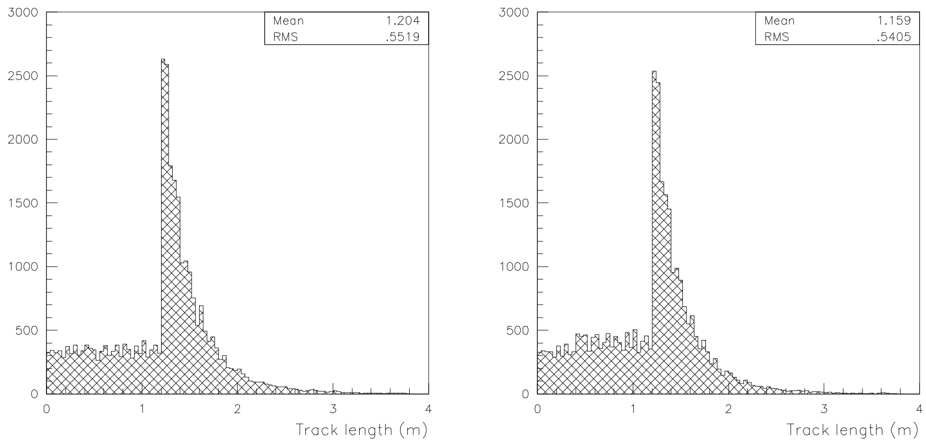

Figure 5: At left the track length distribution for penetrating muons intersecting the detector volume is shown. The right plot is similar except that the muon energy spectrum is now included.

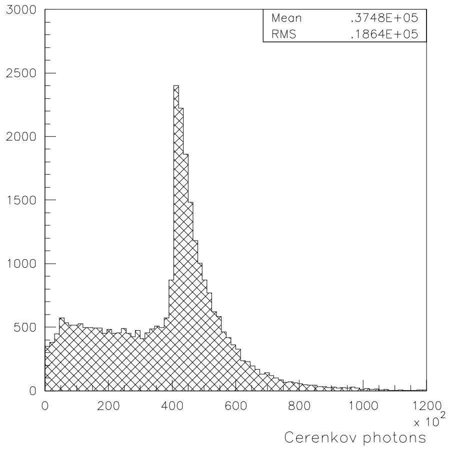

Figure 6: The Čerenkov light pulse amplitude distribution in the tank including muon zenith angle and energy spectrum effects. ($300 < \lambda < 600$ nm.)

for $p < 200$ MeV/c 8% of the incident particles range out within the tank. If dN/dp continues flat to $p = 0$ then this fraction increases to 14%.

5 Light collection to the phototubes

In the next stage of the simulation the Čerenkov photons are ray traced as they reflect from the tank lining until they are absorbed or reach a photomultiplier tube (PMT). AWT1 conforms to the reference design [1] in that it is fully Tyvek lined and is fitted with three 8" PMTs which view the water volume vertically downwards from above. The tubes are equally spaced on a circle of radius 1.2 m, concentric with the detector.

In order to produce results which are directly comparable with the experimental data in GAP-97-025 the peak water absorption length, and PMT gain assumed in the simulation were tuned to produce a good match to the amplitude and shape of the average muon telescope pulse recorded on the same day that the self-trigger data was taken; see [9] for details of this process [1].

[1] A caveat: for the purposes of simulation all three PMTs were assumed to have exactly equal gain chosen to give a best match to the mean of the three real gains (which in reality were a little different).

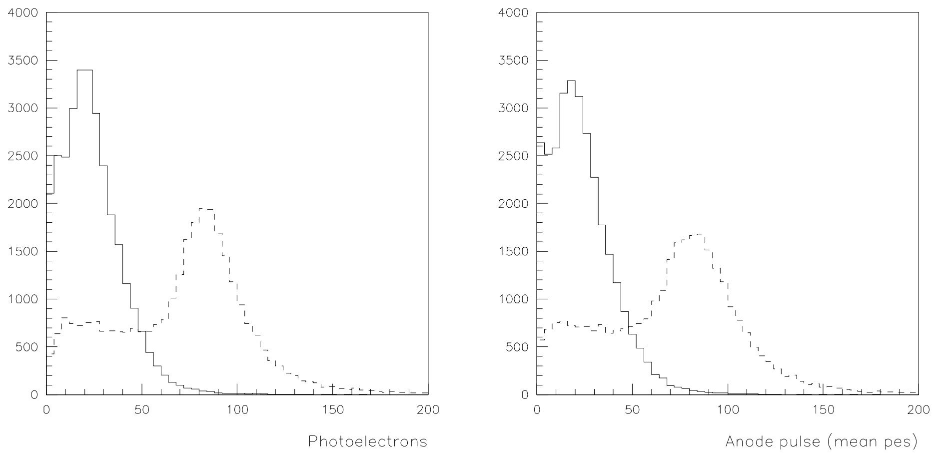

Figure 7: The solid line in the left plot shows the distribution of the number of photoelectrons reaching a single PMT; the dashed histogram is the sum all PMTs. The right plot is similar except that the single electron spectrum has now been included to give anode pulse size.

The solid histogram in the left part of figure 7 shows the distribution of the number of photoelectrons (pes) detected at an individual PMT. The total number of pes on all tubes is also shown as a dashed histogram. Note that the number of pes at *individual* tubes has only a very modest peak to valley ratio.

It has been shown previously by simulation that for a diffusively lined water tank of the proposed Auger design the *total* pe yield over all tubes is rather insensitive to the position at which near vertical muons penetrate the tank [1, 10]. This has been verified several times experimentally [11, 12, 13, 14], and additionally it has been shown that the total signal is proportional to the in-detector track length for non-vertical penetrating muons in most geometries. However the pe yield on each *individual* tube is sensitive to the position at which a muon passes through the tank; this is shown very clearly in reference [14]. Hence figure 7 is not surprising.

6 PMT and electronics simulation

Each pe released from the photocathode produces a fluctuating amount of charge flowing at the anode; an effect known as the single electron spectrum. This is simulated by sampling from an appropriate distribution to derive the sub-pulse size for each contributing pe[2]; the distribution used here is shown in figure 8. The anode pulse size spectrum after folding in this effect is shown in the right part of figure 7.

For the purposes of the current work the front end electronics in use on AWT1 is simulated. Although this does not correspond to the plans for the final Auger surface detector it will certainly be desirable to record calibration data through the same waveform recorder channels that are used for the EAS signals, as is done on AWT1. In this way the performance of the electronics can be monitored, as well as the performance of the tank and PMTs. AWT1 is equipped with a FADC type digitizer making *instantaneous* current measurements every 10 ns (*not* a "time-slice-integrator").

In the simulation the PMT waveforms are constructed and integrated for each muon event taking into account the amplitude quantization of the FADC. The traces are then run through exactly the same analysis code as was used for the real data in GAP-97-025. Figure 9 shows the distribution of the trace integrals for a single PMT and the sum of the three PMTs.

It is in principle possible in a large fraction of cases to separate the prompt light released when non-penetrating muons stop in the tank from that given off by the subsequent decay electrons. The rate of muons intersecting the tank is ≈ 2 KHz, or one every 500 μs. Positive stopping muons decay with roughly the vacuum decay time constant of 2.2 μs, while μ^- frequently undergo atomic capture and decay somewhat faster. Hence the probability for a second muon to enter the tank before the first has decayed is rather small. If in the final design a time stamp is recorded with each calibration trigger, so that the Δt to the next trigger is known, the decay electrons could be rejected, or more probably, used as an additional means of calibration.

In the case of the experimental data in GAP-97-025 10% or more of the triggers may be due to decay electrons, dependent on the trigger condition and threshold. The simulation produces "triggers" from incident muons only; this is a deficiency in the context of the current work.

[2]This distribution was measured for a Hamamatsu R1408 PMT [15] as in use on AWT1. The Auger detectors will probably use modern PMTs with a superior characteristic; however, as we can see, the impact of this effect on the work in hand is not dramatic.

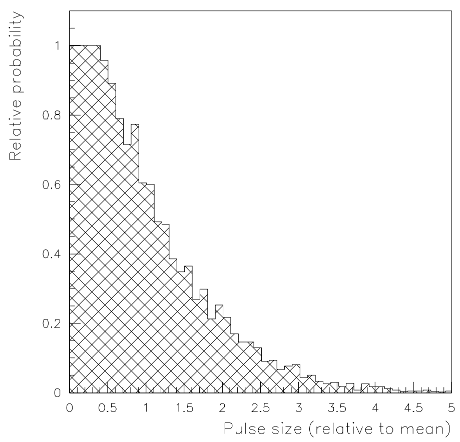

Figure 8: Single photoelectron charge distribution assumed for the purposes of simulation.

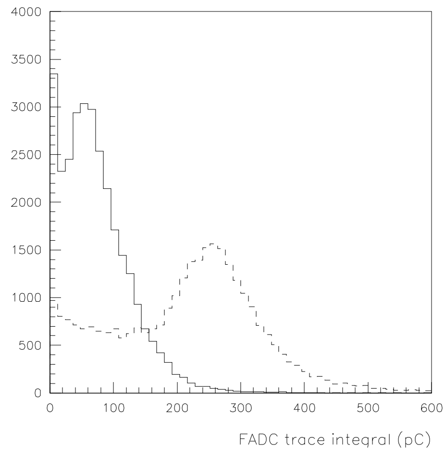

Figure 9: The distribution of FADC trace integrals for a single PMT is shown as a solid line; the sum of all PMTs is shown dashed. All effects are now included.

7 Experimental comparison

It is now in principle possible to simulate the three experimental situations investigated in GAP-97-025 simply be making cuts on a large set of simulated single muon events. Figures 10, 11 and 12 are as close as possible in form to figures 2, 3 and 6 from the previous paper, but display simulated data. Note that the mean and sigma values given are for the Gaussian fit in the peak region of each distribution. Threshold values are given in mV, and the vertical lines show the approximate corresponding pulse charge values.

Qualitatively the real and simulated distributions are similar in all cases. In the case of figure 10 the peak position of the non-trigger tube does not shift with increasing trigger threshold as is observed in the real data. However for the single PMT trigger case of figure 11 the movement of the non-trigger peak positions is consistent with the experimental data.

In each case where disagreement is present it tends to be in the regions of smaller than average and larger than average pulses. Smaller than average pulses will be underestimated in the simulation for two reasons; firstly the softest part of the ground level flux (mostly electromagnetic particles) has been ignored due to lack of data, and secondly DAQ triggers caused by the decay electrons of stopping muons are not included. Larger than average pulses will be underestimated because multi-muon (very small air shower) events are not included.

8 Conclusions

An attempt has been made to simulate the response of the Auger water tanks to the background flux of secondary cosmic rays. Results are similar to the experimental data presented in GAP-97-025, although some limitations of the calculation remain, partly due to lack of knowledge of the nature and energy spectrum of the ground level flux. If anyone reading this knows where more detailed (and accurate!) information can be found please get in touch. This work is primarily an intellectual exercise to demonstrate understanding of the water tank detector. It also serves to validate the simulation code, which can then be used to investigate many aspects of detector performance.

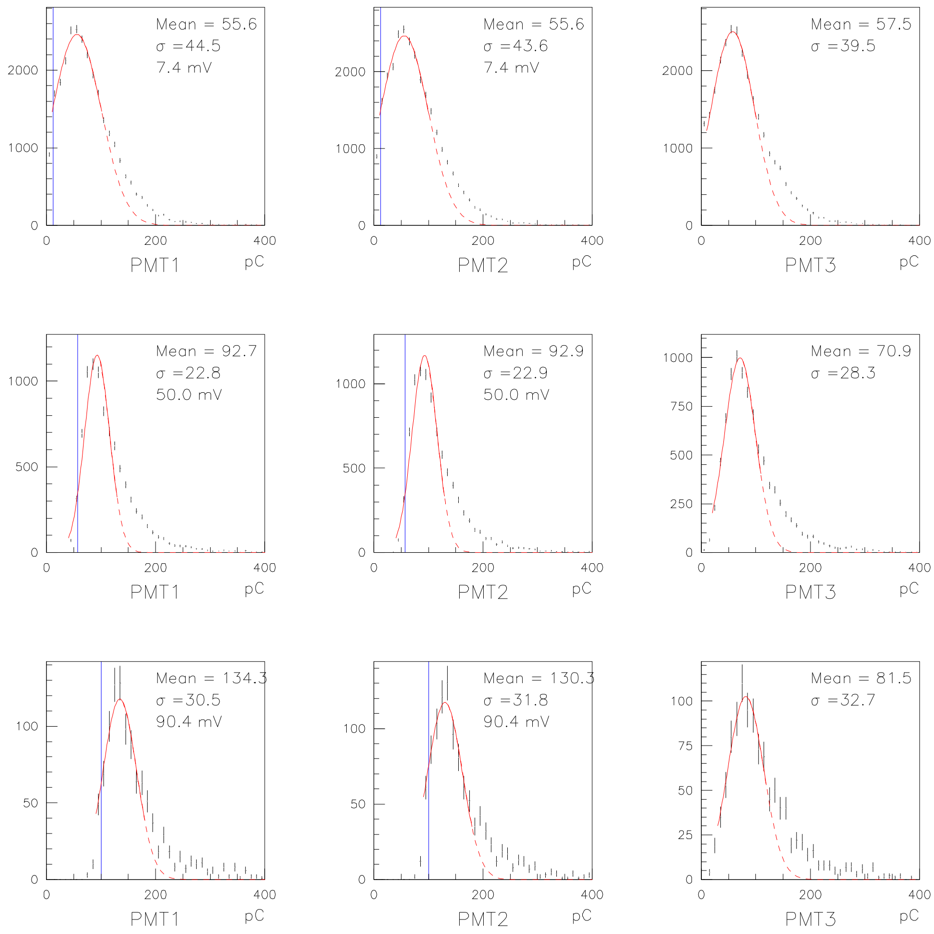

Figure 10: Simulation of AWT1 when triggering on a coincidence of PMTs 1 and 2. The pulse charge distributions of the three tubes are shown at three different trigger thresholds. This figure should be compared to figure 2 in GAP-97-025.

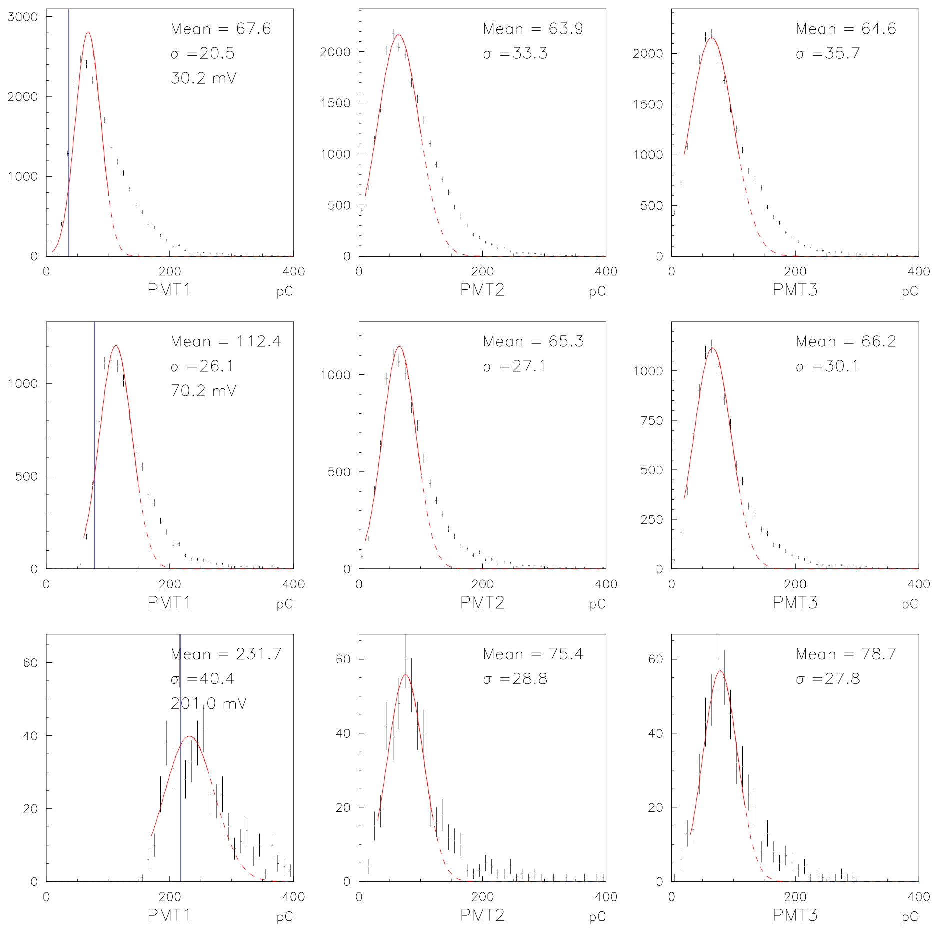

Figure 11: Simulation of AWT1 when triggering on PMT 1 alone. The pulse charge distributions of the three tubes are shown at three different trigger thresholds. This figure should be compared to figure 3 in GAP-97-025.

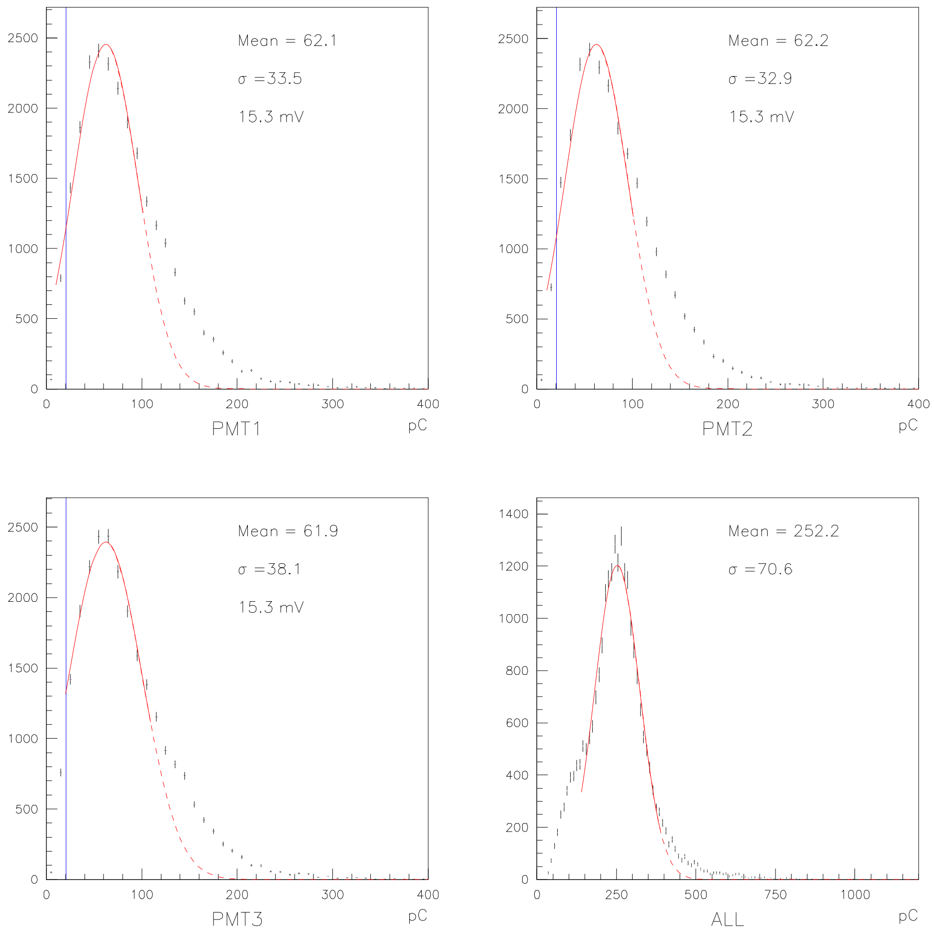

Figure 12: Simulation of AWT1 when triggering on a coincidence of all three PMTs . The pulse charge distributions of the three tubes are shown, with the trigger threshold indicated. This figure should be compared to figure 6 in GAP-97-025.

References

[1] The Auger Collaboration, "Design Report", 1st edition Oct. 1995, 2nd edition Nov. 1996.

[2] T. Kutter, C. Pryke, M. Nagano and N. Sakaki, "Self calibration of the water Cherenkov tanks: Experimental results", Auger tech. note GAP-97-025.

[3] C. Pryke, Auger Ground Array simulation package (AGAsim). (See note below for availability).

[4] N. Sakaki and M. Nagano, "Test of a Water Čerenkov Detector for the Auger Project at Akeno Giant Air Shower Array (AGASA)", *Proc. of the Int. Symp. on Extremely High Energy Cosmic Rays*, ICRR Tokyo, Sept. 1996, page 402.

[5] Particle Data Group, "Review of Particle Properties", *Phys. Rev. D*, **50(3)** (1994) 1269.

[6] T. Gaisser, "Cosmic Rays and Particle Physics", *Cambridge University Press*, (1990) page 71. Reproduced from O. Allkofer and P. Grieder, "Cosmic Rays on Earth", Physics Data Nr. 25-1, *Fachinformationszentrum Karlsruhe*, (1984).

[7] FECyN and Tandar groups, "Simulations with GEANT", Auger tech. note GAP-96-011.

[8] G. Yodh *et al*, "Performance of water Tanks and Igloos", Milagro internal report, Nov. 1996.

[9] C. Pryke, "Performance simulations of a 10 m^2 water Čerenkov detector and comparison with experiment", Auger tech. note GAP-97-004.

[10] C. Pryke, PhD thesis, *University of Leeds*, (1996) page 103.

[11] A. Shih, "Tests of a 6.59 m^2 Prototype Water Čerenkov Detector for the Pierre Auger Project", Auger tech. note GAP-95-014.

[12] D. Ravignani et al, "Studies with a Prototype Water Čerenkov Detector at Fermilab for the Auger Project", Auger tech. note GAP-96-033.

[13] A. Etchegoyen *et al*, "Experience with the Buenos Aires water Cerenkov detector", Auger tech. note GAP-96-040.

[14] N. Sakaki and M. Nagano, "Test of a Water Čerenkov Detector for the Auger Project at Akeno", Internal report, Sept. 1996.

[15] C. Pryke and T. Kutter, "Measurements of R1408 photomultiplier performance", Auger tech. note GAP-96-041.

GAP notes and the Design Report are available from `http://www-td-auger.fnal.gov:82/`.
C. Pryke thesis and AGAsim code is available from `ftp://aupc1.uchicago.edu/pub/auger`.